*Int. J. High Technology Ceramics* **4** (1988) 161–179

# 5

# Uniaxial Tensile Strain Measurement for Ceramic Testing at Elevated Temperatures: Requirements, Problems, and Solutions

K. C. Liu

Metals & Ceramics Division, Oak Ridge National Lab.,
Oak Ridge, Tennessee 37831, USA

H. Pih

Dept. of Engineering Science & Mechanics, University of Tennessee,
Knoxville, Tennessee 37996, USA

&

D. W. Voorhes

Optra Inc., 83 Pine St., Peabody, Massachusetts 01960, USA

## NOTATION

| | |
|---|---|
| $A$ | Complex amplitude of light beam at detector. |
| $A'$ | Complex conjugate of $A$. |
| $A_0$ | Absolute value of $A$. |
| $a$ | Distance between the edges of gap-opening. |
| $\Delta a$ | Change of the gap-opening. |
| $I$ | Intensity of radiation field at the light detector, $I = A \times A'$. |
| $\langle I \rangle$ | Intensity of the light scattered by each scattering site. |
| $I_N$ | Intensity resulting from the interference of light scattered from two incident beams. |
| $I_0$ | Absolute value of $I$. |
| $I_s$ | Random variable with an rms value of square root of $N$. |
| $i$ | Imaginary unit, the positive square root of $-1$. |
| $L$ | Gage length of strain extensometer. |
| $N$ | Effective number of independent scattering sites. |

| | |
|---|---|
| $n$ | Number of interference fringes passing through a detector aperture. |
| $R$ | Distance between the gap and detector. |
| $S$ | Spacing between adjacent fringes. |
| $x$ | Displacement of fiducial point in measurement direction. |
| $\Delta x$ | Extension between the gage length $L$. |
| $\theta$ | Angle between the incident and reflecting light. |
| $\lambda$ | Wavelength of monochromatic light source. |
| $v$ | Frequency of light. |
| $\Delta v$ | Laser frequency difference. |
| $\Phi$ | Change in phase between two beams of light. |
| $\chi$ | Offset of the detector from the centre of the light beam. |

## 1 INTRODUCTION

Advanced ceramics offer great potential in many engineering applications at temperatures above 1000°C. The mechanical properties such as true tensile strength, modulus of elasticity, fatigue and creep behaviour of the ceramic materials at high temperatures are important to designers in order to set design stress limits and to establish methods of predicting lifetime. Unfortunately, the database needed for the design purposes is practically nonexistent. Reasons for the scarcity of the information can be attributed to many experimental difficulties inherent in testing brittle materials in hostile environments and at high temperatures.

To establish the design database, the complex relationships among the following three variables must be characterised: stress (or strength), strain (or deformation), and temperature. Significant progress has been made in recent years in the development of tensile testing methods to determine the true strength of ceramic materials. The objective is to apply uniform stress to the tensile specimen. Several experimental efforts can be cited: Soma *et al.* (1985), Nilsson & Mattsson (1986), Liu & Brinkman (1986, 1988) and others.

In contrast, significant progress has not been made in the development of strain measurement techniques for high temperature testing. There are several reasons. First, the strength property has always been a major concern to ceramic engineers, whereas the importance of strain property has always been low in priority. However, this has changed since advanced ceramics were introduced as potential structural materials. Second, strain measurement is immensely difficult to conduct in hostile environments using conventional methods for various reasons. Third, uniform stressing of the specimen is also a concern in uniaxial strain measurement because most high

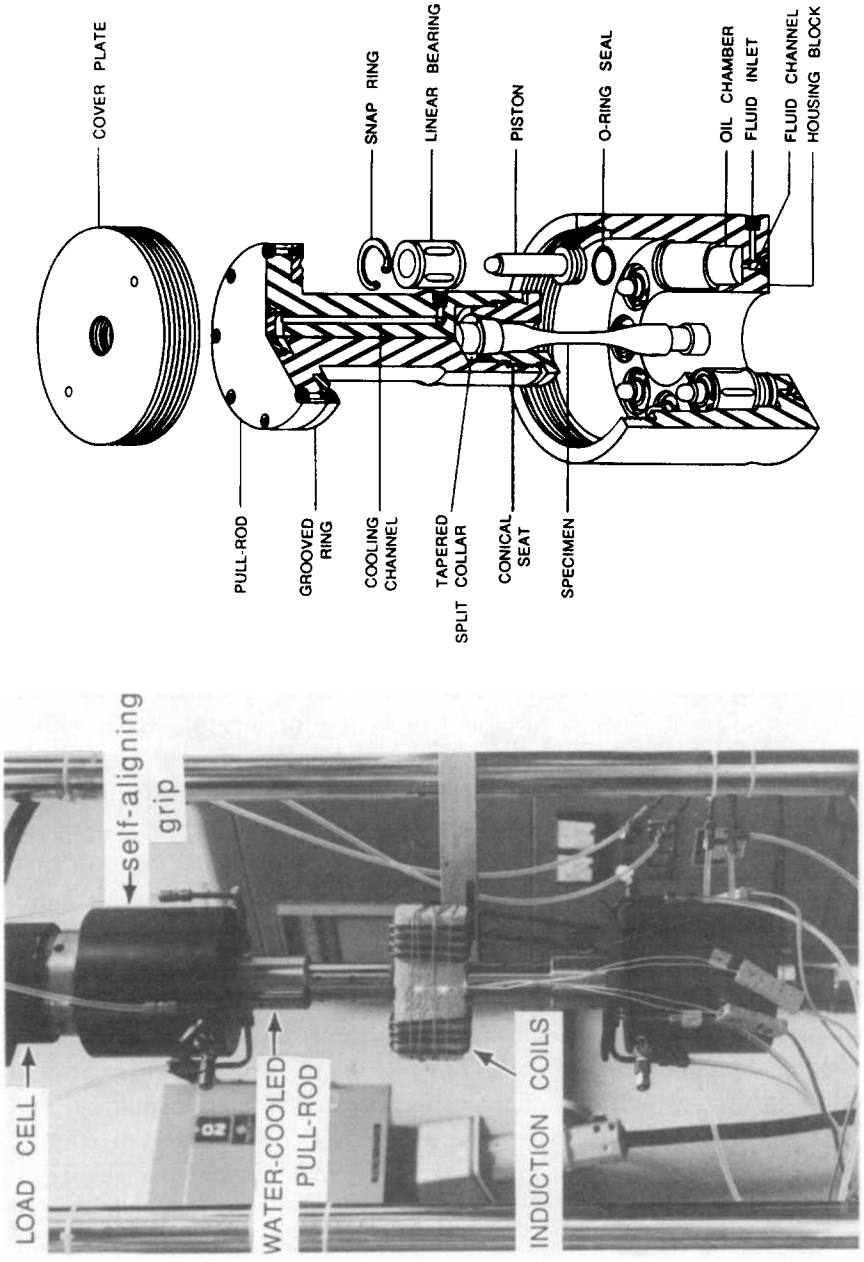


**Fig. 1.** Load-train column assembly installed on universal testing machine for tensile testing of ceramic specimen at 1200°C using induction heating method (left); details of ORNL-developed hydraulic operated self-aligning grip for ceramic testing in true tension (right).

temperature strain extensometers measure strain on one side of the specimen surface. Uniform stressing in tension can now be achieved using the ORNL-developed gripping system which operates hydraulically with a self-aligning feature, as shown in Fig. 1.

To complete the full testing capability, we are currently focusing our efforts on the development of strain measurement techniques for applications to high temperature testing of ceramic specimens. The purpose of this paper is to describe the extensometers that are under development at ORNL and to cite results generated with these strain extensometers so that their effectiveness can be assessed. Temperature measurement will not be discussed here because it falls outside the scope of this paper.

## 2 STRAIN MEASUREMENT REQUIREMENTS

The value of foil strain gages as a means for strain measurement needs no further introduction, as long as the use is limited to ambient temperature. The accuracy of strain measurement by the foil strain gages appears to surpass that of other methods. Foil strain gages offer a high degree of precision; in the order of a few microstrain. A microstrain is defined as $10^{-6}$ m/m. Better than 1 microstrain resolution is possible depending on the sensitivity of the instrument used. However, at the present time there are no resistance strain gages suitable for use at temperatures above 1000°C. In such situations, the strain measurement must rely on strain extensometers which may be classified in two characteristically different groups: mechanical and optical. The mechanical strain extensometers are usually placed in contact with the test specimen via mechanical extenders which reproduce the strain change and transfer it to an external transducer. In contrast, noncontact is a unique feature of the optical strain extensometer, although small fiducial marks (called reference marks) are needed as targets on the tensile specimen, except in some cases.

Strain extensometers with accuracies in the range of 30 to 80 microstrain with a 5 to 10 microstrain resolution, equivalent to B-1 classification of extensometer systems specified in ASTM E83 (1985), are suitable for use in high temperature testing of engineering ceramics. The accuracy and resolution are usually governed by factors such as operational principles, degree of complexity in extension mechanisms, and sensitivity of detecting transducers used in the systems. A comparison of this performance to that of the strain gage clearly indicates that extensometers generally underperform the strain gages by a substantial margin. However, many strain extensometers are still adequate for the purpose of generating engineering data.

Strain measurements for three modes of tensile testing are of general interest here. They are tensile fast fracture; dynamic cyclic fatigue; stress-rupture and time-dependent deformation (creep). Unless dealing with superplastic materials, much of the tensile test data on fracture strain of ceramic materials will be less than 0·5%. A calculation will show that the potential error in the test data resulting from using an extensometer system with an average measurement error of $\pm 55$ microstrain is less than 2·5% of the full strain measurement range. An error below 5% is considered acceptable for most engineering applications.

Strain measurement for dynamic cyclic fatigue testing may require an extensometer with a higher degree of accuracy than that used for tensile fast fracture testing. Using the ORNL fatigue data generated by Liu & Brinkman (1988) as a guide, we estimate that some cyclic fatigue tests may be run to a cyclic strain amplitude as low as 0·12%. Applying the same 5% error criterion, we can show that the extensometer to be used in this test must perform with accuracy better than $\pm 30$ microstrain.

Also, it can be shown that a less stringent strain extensometer is apparently acceptable for tensile stress-rupture testing (creep testing), provided that the extensometer system has a greater strain measurement range to work with. With reference to Cannon & Langdon (1983), steady-state creep deformations end at about 2–3% or less for ceramic materials of general interest. Using the same criterion, the accuracy requirement of the strain extensometer can be relaxed to about 100 microstrain. However, unlike the preceding cases where the relative accuracy is important, the absolute accuracy is critical to the creep strain measurement.

## 3 MECHANICAL STRAIN EXTENSOMETERS

Mechanical strain extensometers have been widely used in tensile testing of metals for many years because they can be made inexpensively and yet give satisfactory results. Simplicity, economy, and good accuracy of these devices are the reasons why foil strain gages are not used so much in uniaxial tensile testing except for aligning the specimen and load train. Several types of strain extensometers are commercially available. However, most of them are usable only in low temperature conditions; only a few are applicable for ceramic testing at temperatures above 1000°C. Nevertheless, these devices still suffer from some restrictions. The major problem is to secure the extensometer on the ceramic specimen so that slippage does not occur at the contact points, which in most cases are also the fiducial points. On the other hand, applying excessive pressure on the contact points may introduce irreparable damage to the surface of the specimen.

The basic design concept used in the mechanical extensometers are in principle about the same. An elastic hinge or scissor-like design is most common. The accuracy of mechanical extensometers generally falls in the range of 30–60 microstrain, depending on the measuring range, service temperature, and the accuracy of transducers. With reference to earlier discussions, it appears that most mechanical strain extensometers are adequate for tensile strain measurement.

### 3.1 Details of ORNL strain extensometer

A high temperature strain extensometer developed at ORNL and shown in Fig. 2 is currently being used for ceramic specimen testing in our laboratory. An error analysis indicates that it has an accuracy of about 25–30 microstrain with a 5 microstrain resolution. It is a biaxial (tension–torsion) strain extensometer specifically developed for testing a tubular specimen

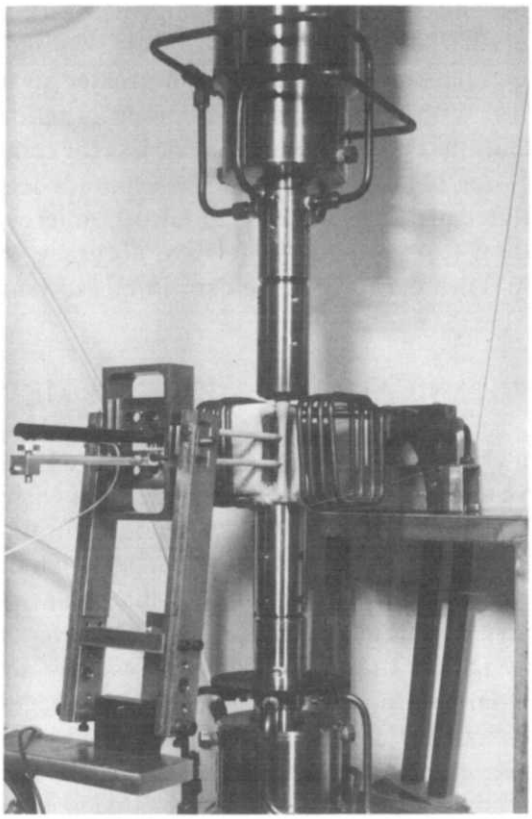

**Fig. 2.** High temperature mechanical strain extensometer installed on a ceramic specimen at the test position.

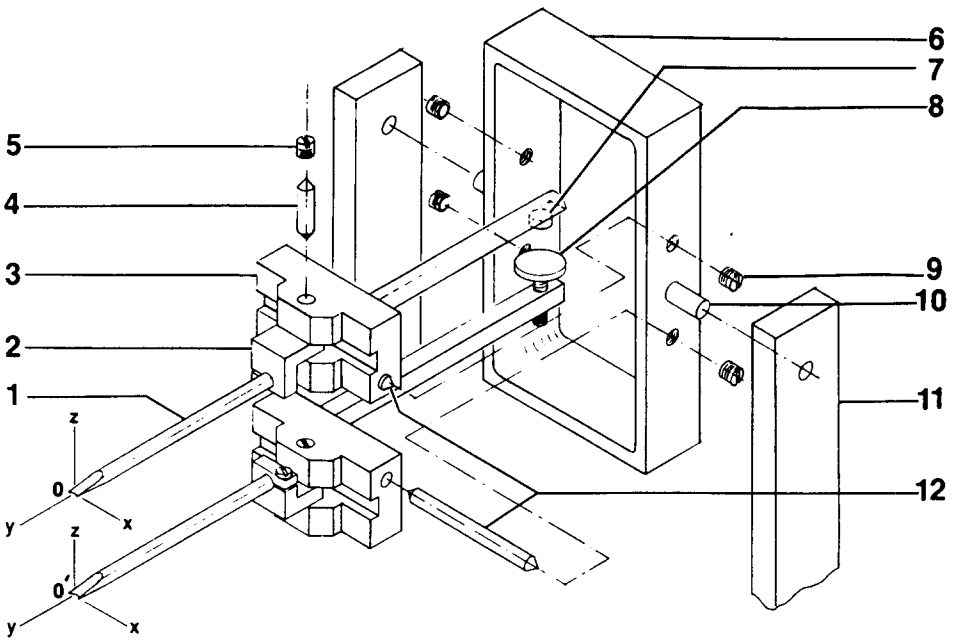


**Fig. 3.** Details of ORNL mechanical strain extensometer for ceramic testing at high temperature.

subjected to combined tension–torsion loading. The details are shown in Fig. 3. The torsion transducers are removed from the extensometer for uniaxial applications.

The basic elements of the extensometer are two assemblies of universal joints (3). Each assembly has two independent orthogonal axes (4 and 12) of rotation so that the tip of the ceramic probing rod (1) can follow the displacement of the fiducial point 0 on the X-Z plane. The probing rod, made of high purity aluminium oxide, is attached indirectly to the short vertical shaft (4) by a small angle block (2). The ends of the horizontal shaft (12) are supported at the jambs of a rectangular frame (6) which in turn is supported by a freestanding bracket (11). To obtain accurate strain measurements, close articulations are essential between the shaft and the end supports. To accomplish this, both shafts are tapered at the ends and supported by a pair of matching countersunk brass screws (5 and 9). With proper adjustment of the screw pressure the shafts can rotate freely.

The extensometer is completed with a small lightweight capacitive transducer (7) which is attached to the upper extension bar. Placed directly underneath the transducer is a circular flat-headed ground plate (8) which is attached to the lower extension bar by a screw for gap adjustment. The differential displacement occurring at the tips of the probing rods is

proportionally reproduced at the far end of the extension rods in terms of the change in the air-gap.

### 3.2 Operation and test results

Figure 2 shows the strain extensometer installed in the test position. The contacts between the specimen and probing rods are controlled by a light horizontal thrust force due to the weight of the extensometer itself and the supporting bracket leaning forward to the specimen. To maintain firm but light contacts on the specimen surface, care must be exercised. The best result is obtained when the probing rods are inserted perpendicular to the specimen, because the thrust force imposed on the rectangular frame is then distributed evenly to each probing rod. Figure 4 shows sample results obtained using the ORNL strain extensometer.

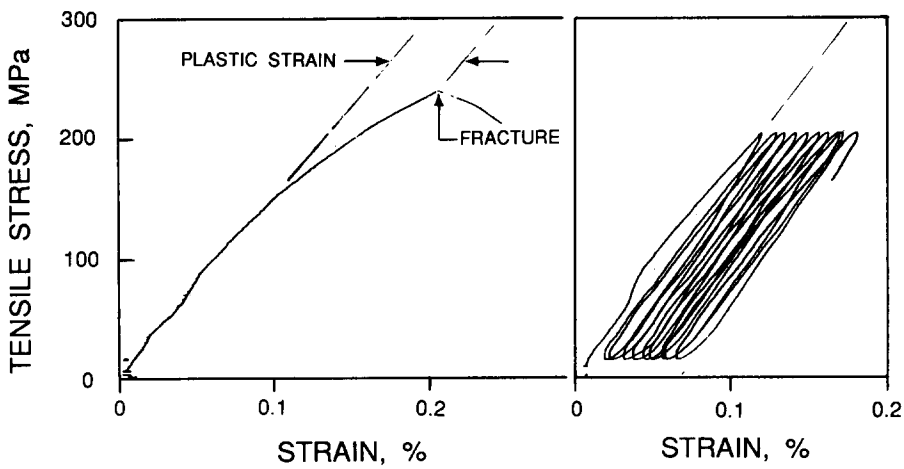


**Fig. 4.** Stress–strain diagram for silicon nitride tested at 1200°C using the mechanical strain extensometer: monotonic tensile loading to fracture failure with a hint of slight plastic deformation at the end of the test run (left); strain ratcheting, i.e. incremental accumulation of plastic strains, resulting from tension–tension cyclic fatigue loading at high temperature (right).

## 4 OPTICAL STRAIN EXTENSOMETER

The most serious weakness of the mechanical extensometer is the contact problem as discussed in the preceding section. Therefore, the measurement by noncontact optical means has been the subject of extensive research. Optical strain extensometers offer a wide range of accuracy to suit various measurement requirements. The sensitive end of the range could reach as

low as $\pm 5$ microstrain and the opposite end of the spectrum to $\pm 100$ microstrain.

The micrometer-based optical extensometers have been used to measure creep strains with a precision of about $\pm 100$ microstrain and a resolution of about 10 to 20 microstrain. In contrast, the advanced optical system uses the coherent light wave as the reference measurement scale so that the accuracy improves dramatically by a factor of 10–20. This section is intended to acquaint the reader with a simple, low-cost, laser-based diffractive optical extensometer and a state-of-the-art two-frequency laser extensometer.

## 4.1 Diffractive optical strain extensometer

Two optical methods, utilising the diffraction of collimated light passing through a narrow slit, have been developed. The first method relates the change in distance between the two edges of the slit to the movement of the diffraction-produced fringes. The resolution of this method is governed by the techniques used to interpolate the nonlinear characteristics of the light intensity appearing between half order fringes. The second method is based on the relationship between the gap width of a single slit and corresponding fringe spacing. The accuracy of the method depends upon the accuracy of the measurement of the fringe spacing which can be improved through instrumentation.

### *4.1.1 Optical theory*

When a beam of collimated monochromatic light passes through a narrow slit, the light waves diffracted by the edges produce an interference fringe pattern in the form of bright and dark bands parallel to the slit, as illustrated in Fig. 5. This phenomenon is known as Fresnel diffraction. If a small aperture of a photodetector is placed at an offset distance $\chi$ from the centre of the beam and a distance $R$ from the slit as shown in Fig. 5, the number of fringes moving past the aperture is related to the change of the gap opening. The basic principle is similar to that used by Sharp (1971). This relationship can be approximated by the following equation:

$$\Delta a = (n)\ R\lambda/\chi \tag{1}$$

If two short bars with one end of each bar bevelled and the other, straight end, cemented to the specimen as shown in Fig. 5, the change of the gage length $L$ is measured between the cemented points. The average strain is calculated from the changes of gap width $\Delta a$ with respect to $L$.

Another method using a similar arrangement was developed. This method is based on the fact that the gap opening $a$ is related to the spacing

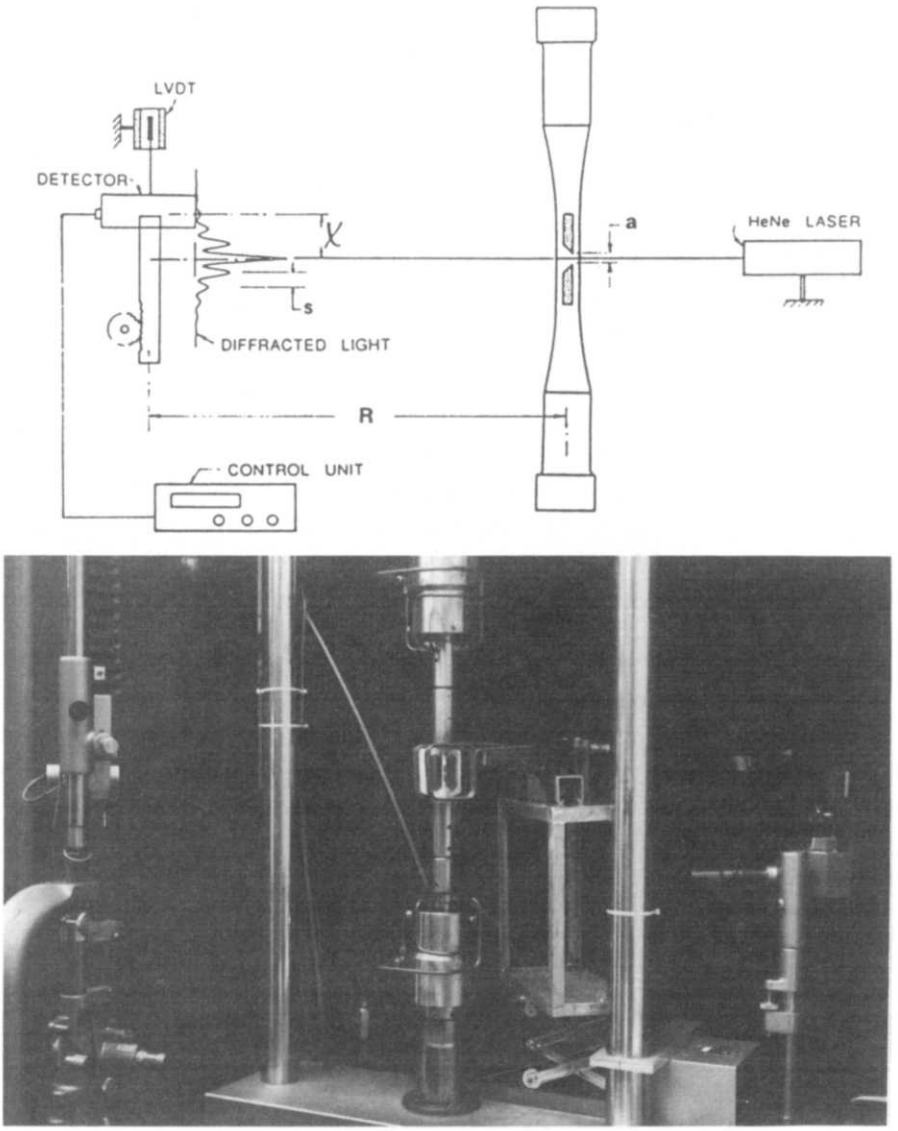


**Fig. 5.** Schematic diagram illustrating the basic configuration of diffractive optical strain extensometer (top); arrangement of the optical strain measurement system at the test position (bottom).

between adjacent fringes $S$ by the following equation for Fresnel diffraction of a single slit, given by Jenkins & White (1976):

$$a = R\lambda/S \tag{2}$$

This method requires moving the detector across the diffraction patterns for each measurement run.

The two methods are used for different measurement objectives. The first is used for dynamic or static strain measurements, whereas the second method is mainly used for static or long-term measurements in conditions such as creep.

*4.1.2 Instrumentation*

For both methods, the basic instrumentation is the same. The light source is a 2-mW He–Ne laser which produces a well-collimated light beam of 2 mm in diameter with a wavelength of 633 nanometers. The laser tube is mounted on cross slides which provide vertical and horizontal movements to align the light beam with the slit.

The gap is formed by two pieces of short rectangular ceramic bars. One end of each bar is ground to a 45° bevel and the square ends are cemented to the ceramic specimen with Aremco 569 high temperature ceramic adhesive, which cures at room temperature.

The detector consists of a photocell mounted in a metal tube, the front end of which has a cover with a small aperture at its centre. The detector is mounted on a support attached to a vertical slide and vernier to read the vertical movement of the detector to 0·0025 mm. Independently, a linear variable differential transformer (LVDT) attached to the slide is used to cross-check the vernier reading. In the second method, the vertical slide movement is driven by a stepper motor for scanning the fringe pattern, and the fringe spacing is measured by the LVDT. Both the bias voltage to the detector and its output voltage are conditioned by the control unit. The output of the detector is related to the light intensity across the fringes and has a form similar to a sinusoidal curve.

The detector output is related directly to the change in gap width in the first method. The light intensity versus the load or the displacement is recorded by an $XY$ recorder with one axis indicating the detector output and the other the load or displacement. The load is measured by a load cell and the displacement by the LVDT.

*4.1.3 Experimental verification and calibration*

To test the validity of the methods and to establish their accuracy, calibration was carried out in our laboratory. For testing the first method, two thin nickel strips bent into an L-shape were fixed on the side of a flat tensile specimen made of a special aluminium alloy with a very high yield point. A resistance strain gage was cemented on each side of the specimen. In the first method the reference gap size is not a variable in eqn (1). However, as seen from eqn (2), the smaller the gap the larger is the fringe spacing. If the gap is extremely narrow, only a few fringes with very large spacing can be obtained. This produces a noisy signal that makes the determination of the

peaks and valleys difficult, hence there is a loss of accuracy. On the other hand, a large gap produces dense fringes that are difficult to recognise through the narrow slit used to mask the photocell. A gap size of about 0·127 mm is acceptable.

A tensile test was performed for the strain-gaged specimen with the optical strain extensometer described above. Results showed that the strains calculated from the diffraction gage measurement using eqn (1) and that from the strain gages agreed reasonably well. Differences from 6 to 15% based on the strain gage data were obtained. Note that the strain gages measured the local strain, whereas the extensometer measured the average strain over the gage length. For testing the second method, we first investigated the validity of the relationship between the gap size and the fringe spacing. The gap opening was formed by two straight edges mounted on a micrometer-driven slide, one on the stationary frame and the other on the moving frame to provide variable gaps. The micrometer readings for different gap sizes including that for zero gap were calibrated with a travelling microscope. The zero-gap reading was double-checked by extrapolating from the relation between the gap opening and micrometer readings. The intensity of the diffracted light was scanned by the detector mounted on a hydraulic ram rod which travelled vertically. The travel of the ram was measured by an LVDT.

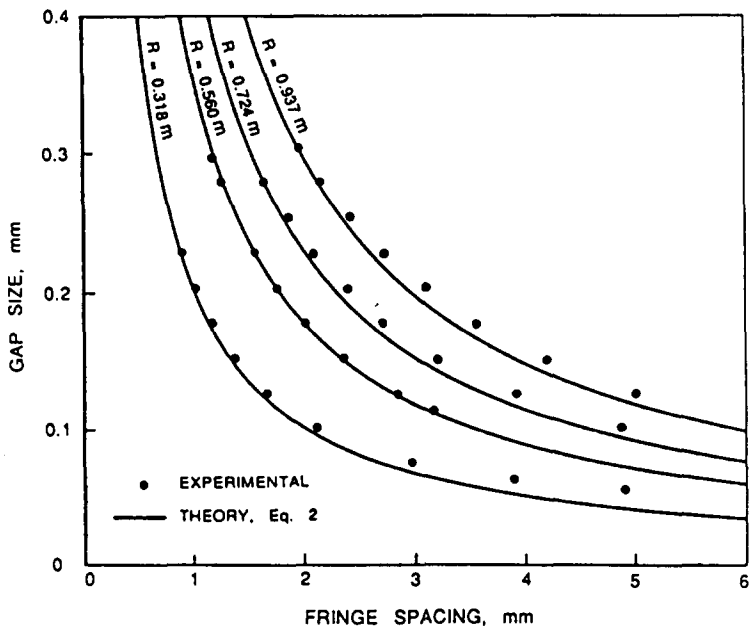


**Fig. 6.** The relationship between the target gap opening and spacing of equispaced interfering fringes formed by diffraction of incident light.

Spectra of the light intensity across the diffraction fringes were recorded for various combinations of prescribed gap size and the distance between the gap setting and the detector; as many as necessary to verify eqn (2). The spacing, $S$, between the adjacent peaks or valleys was measured from the graphs recorded during the scanning. The results are plotted in Fig. 6 which shows the relationship between the gap opening and the spacing of equispaced interfering fringes. All the curves form the shape of a hyperbola, as predicted by eqn (2). Reasonably close agreement between theory and experiment is demonstrated.

*4.1.4 Test results*

A preliminary test was performed on a stainless steel specimen instrumented with a foil strain gage. The gap fixture was made with a pair of L-shaped metal strips as described earlier. Test results are shown in Fig. 7. Except for the strain measurements taken at the end of the first step loading which showed a major discrepancy, the optical extensometer clearly demonstrated the strength of strain measurement by the diffraction method.

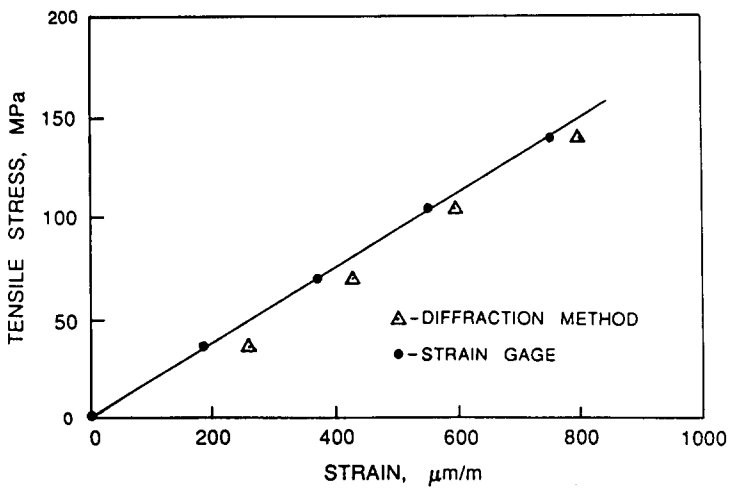


**Fig. 7.** Comparisons of strain measurements by strain gage and the diffraction strain extensometer for a stainless steel specimen subjected to tensile loading.

## 4.2 Two-frequency laser extensometer

Optra Inc. has recently introduced a two-frequency laser extensometer which is ideally suited for noncontact, high temperature applications. It provides a precision of $\pm 5$ microstrain, and, depending on system configuration, an unlimited dynamic range. Strain measurements have been

successfully accomplished at 1100°C; and, with appropriate optical and spatial filtering, temperatures approaching 1650°C and higher are possible.

The first field test was performed at ORNL in March 1987 on a niobium test sample in high vacuum at 1100°C. Subsequent improvements have extended the capability of the extensometer to open-air testing as well as a broader range of materials including ceramics.

### *4.2.1 Optical theory*

The laser extensometer works by measuring the $x$-displacement of a surface at two points whose $x$-coordinates differ by the gage length, $L$. The difference between the two displacements is the extension of the surface for the gage length. The means by which the $x$-displacement of the surface at either point is measured is illustrated in Fig. 8. In Fig. 8(a), a beam of light is incident from the left on a diffusely reflecting surface at an angle $\theta$. The light is scattered upward along the normal of the surface. If a scattering site on the surface moves a distance $x$ from $P_1$ to $P_2$ then the light must travel an extra distance $x \sin \theta$ from the source to reach the detector. Conversely, if a second beam of light is incident from the right at angle $\theta$, as shown in Fig. 8(b), the optical path will be shortened by the same amount by $x \sin \theta$. If both beams come from the same source, as shown in Fig. 8(c), the net difference between their optical paths is thus changed by a distance $2x \sin \theta$ due to the in-plane

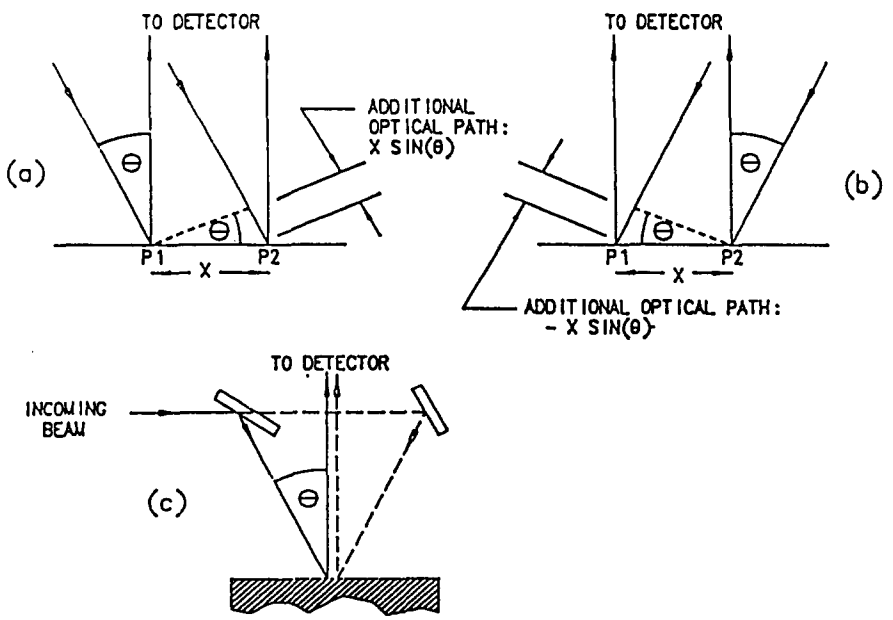


**Fig. 8.** Method of optical detection of in-plane displacement.

$x$-displacement of the surface. The corresponding change in phase between the two beams of light is given by:

$$\phi = (2\pi/\lambda)2x \sin\theta \tag{3}$$

Theoretically, the in-plane displacement $x$ of the surface may be inferred from the phase change $\phi$, which is observable directly by interfering the two beams.

If the scattered components from the two beams are assumed to have the same magnitudes, and to have very nearly equal frequencies $v_1$ and $v_2$ then the complex amplitudes of the two beams at the detector can be written as:

$$A_1 = A_0 \exp(2\pi i v_1 + \phi/2) \tag{4a}$$

and

$$A_2 = A_0 \exp(2\pi i v_2 - \phi/2) \tag{4b}$$

In terms of the sum of these two amplitudes, $A \equiv A_1 + A_2$, the intensity of the radiation field at the detector is given by:

$$I \equiv\equiv A \times A' = 2I_0 [1 + \cos(2\pi\Delta v t + \phi)] \tag{5}$$

where $I_0 \equiv A_0^2$. In conventional interferometry, the two frequencies $v_1$ and $v_2$ are the same and $\Delta v$ is zero. In this case, eqn (5) becomes:

$$I = 2I_0 + 2I_0 \cos\phi \tag{6}$$

and the phase $\phi$, which is proportional to the in-plane displacement of the surface $x$, must be deduced from an essentially DC intensity measurement in the presence of a background level. In fact, the problem is more difficult to resolve, as described in detail by Hercher *et al.* (1987), because a real measurement with a diffusely reflecting surface entails scattering by many randomly phased independent scattering sites.

The intensity resulting from the interference of light scattered from the two incident beams can be shown to have the form

$$I_N = N\langle I\rangle_0 + I_s \cos\phi \tag{7}$$

The net result of the complications arising from dealing with a real diffusely reflecting surface is that $\phi$ cannot be reliably inferred from a low-frequency intensity measurement; the fluctuating background intensity level is too high in comparison with the intensity of the component which is proportional to $\cos\phi$.

Optra's solution to this problem was to introduce the use of a stabilised two-frequency He–Ne laser. Its output is comprised of two orthogonally polarised, collinear components which differ in frequency by exactly 250 kHz. Figure 9 shows an arrangement by means of which the two-frequency components can be made to illuminate the surface in the desired

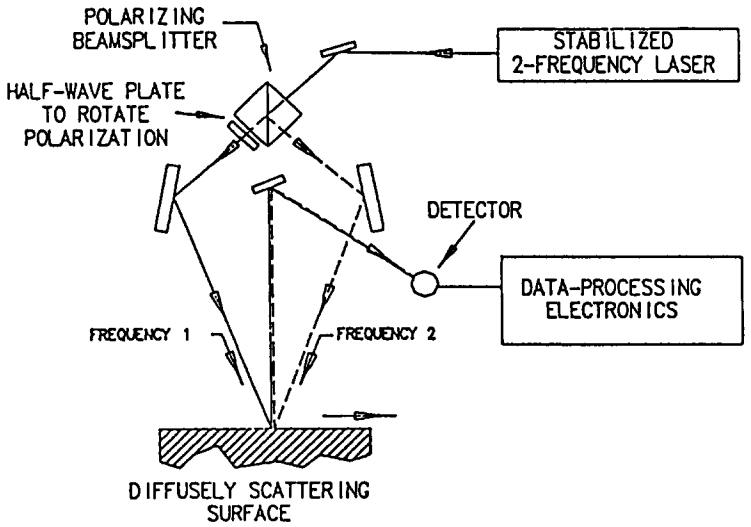


**Fig. 9.** In-plane displacement measurement by a two-frequency laser.

manner. The light intensity due to the interference between the two scattered beams, taking into account the random nature of a diffusely reflecting surface, can be written as:

$$I = N\langle I\rangle_0 + I_s \cos(2\pi\Delta\nu t + \phi) \tag{8}$$

where $\Delta\nu$ is the laser frequency difference (250 kHz). The critical point is that $\phi$ is now manifest as the phase of the 250 kHz modulation frequency, rather than as a change in intensity level. Because of this, the intensity level, together with any low-frequency fluctuations in the intensity level, can be easily eliminated from the signal by the simple expedient of coupling (high-pass filtering). This allows reliable, accurate, and rapid noncontact measurements of the in-plane displacements of diffusely scattering surfaces.

*4.2.2 System layout*

The Optra laser extensometer system consists of three main components: the OPTRLITE two-frequency laser, the sensor head, and an electronic phasemeter, as shown in Fig. 10.

The sensor head, which is mounted directly to the OPTRLITE laser, splits this laser beam into two separate pairs of interfering beams, each pair corresponding to a separate measurement spot on the sample surface. The reflected signals from each of these measurement spots are then transported via fibre-optic cables to the phasemeter, where they are converted to electrical signals. The phasemeter calculates the displacement which has occurred at each measurement spot and then determines the extension by

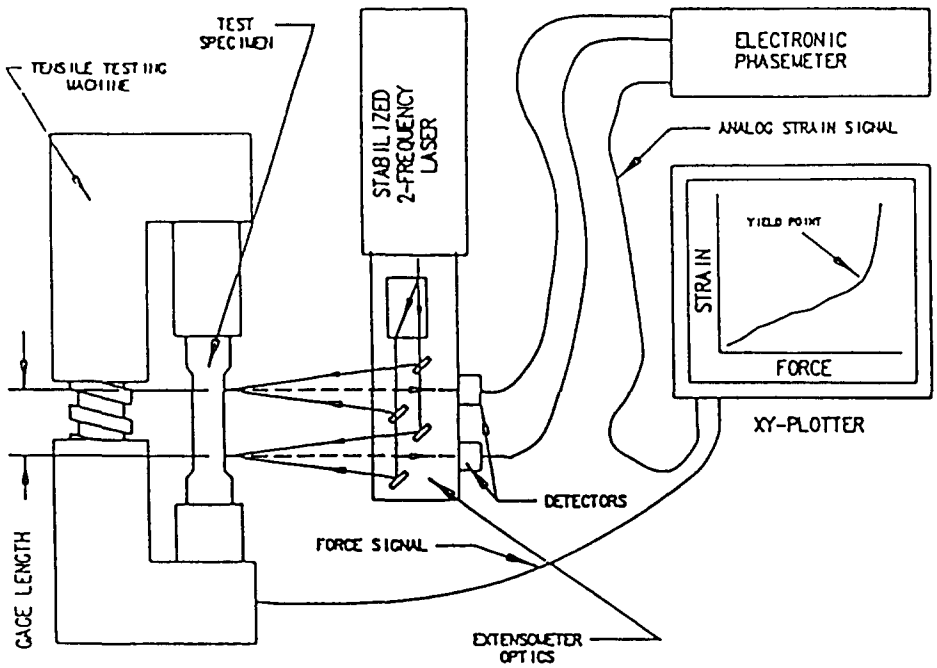


**Fig. 10.** Schematic diagram of Optra's noncontact laser extensometer.

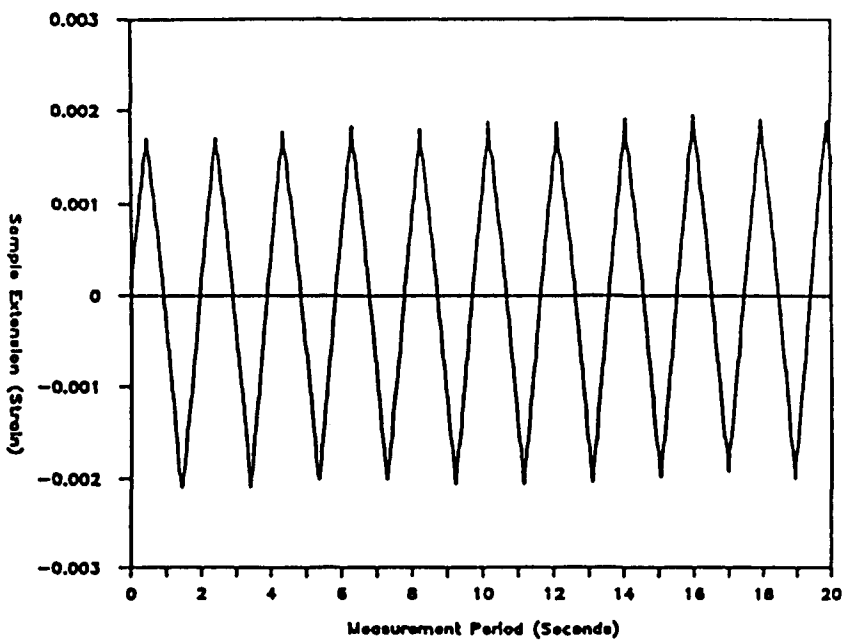


**Fig. 11.** Stress–strain diagram of fully reversed cyclic fatigue test on a dark alloy sample at 538°C and cycled at 0·5 Hz. The test was performed in air.

subtracting these displacements from one another. An analogue signal corresponding to the strain of the sample is then output by the phasemeter.

In the Oak Ridge field test configuration, the phasemeter worked in conjunction with an IBM PC. The disadvantage of the PC approach is that the update rate of the system, which is 100 Hz in this case, is limited by the processing speed of the computer. Optra is developing a phasemeter in which the signal processing is done entirely in hardware. These systems are much faster and can provide update rates approaching 62·5 kHz, well suited for high frequency, servo-loop control applications.

*4.2.3 Results*

The Optra laser extensometer has been demonstrated on a variety of different materials ranging from shiny metals to ceramics. The graph depicted in Fig. 11 is typical of the results that can be obtained with this system. In this testing condition, a low emissivity metallic sample at 538°C was cycled at approximately $\pm 0{\cdot}2\%$ strain at 0·5 Hz.

## 5 SUMMARY

Requirements for strain measurement on tensile ceramic specimens at high temperatures were examined for three test conditions including monotonic fast fracture, cyclic fatigue, and long-term stress-rupture tests. Results indicate that existing extensometers capable of accuracy between 30 and 80 microstrain are adequate for use in the tests to generate meaningful engineering design data. Accuracy better than 30 microstrain is desirable for the first two test conditions, whereas the accuracy requirement can be relaxed to about 100 microstrain for the third one. However, long-term stability and better absolute measurement accuracy needed for the third test condition cannot be compromised.

The theory, design, and use of a mechanical and two optical strain extensometers have been described. Results obtained from tensile and fatigue tests at 1200°C show that the technique using the ORNL mechanical extensometer is effective. However, the extent of its effectiveness may be severely restricted by failure to maintain reliable contact with the specimen as temperature and test frequency increase. Noncontact, good stability, and the precision of well-defined coherent light waves are the bases for the development of the diffractive optical strain extensometer. Comparisons between the results of a control test and companion data obtained by a strain gage shows that the accuracy of the system for strain measurement far exceeds the requirements for creep testing. The Optra optical strain extensometer, based on a two-frequency He–Ne laser, has been demonstrated to provide high sensitivity, large dynamic range, large measurement

bandwidth, and ease of operation. The technique is effective for a variety of metallic as well as ceramic specimens having a diffusely reflecting surface.

## ACKNOWLEDGEMENTS

This work was supported by the US Department of Energy (DOE), Assistant Secretary for Conservation and Renewable Energy, Office of Transportation Systems, as part of the Ceramic Technology for Advanced Heat Engines Project of the Advanced Materials Development Programs, under contract DE-AC05-840R21400 with Martin Marietta Energy Systems, Inc. The development of the two-frequency laser extensometer was funded by DOE under SBIR contract No. DE-AC02-84ER80182 and NASA under SBIR contract No. NAS3-24848.

The authors wish to thank Dr Michael Hercher (Optra) for his contribution to the optical theory (section 4.2.1), Drs W. A. Simpson and M. K. Ferber for reviewing the manuscript, C. O. Stevens for his assistance in performing the experiments, and Billie Russell for preparing the final manuscript.

## REFERENCES

ASTM E83 (1985). Standard practice for verification and classification of extensometers. *Annual Book of ASTM Standards*, 03·01, 272–9.

Cannon, W. R. & Langdon, T. G. (1983). Review: creep of ceramics, part I, mechanical characteristics. *J. Mater. Sci.*, **18**, 1–50.

Hercher, M., Wyntjes, G. & Deweerd H. (1987). Non-contact laser extensometer. In *Proceedings of the International Society for Optical Engineering*, **746**, 185–91.

Jenkins, F. A. & White, H. E. (1976). *Fundamentals of Optics*, McGraw-Hill, New York.

Liu, K. C. & Brinkman, C. R. (1986). Tensile cyclic fatigue of structural ceramics. In *Proceedings of the 23rd Automotive Technology Development Contractors' Coordination Meeting*, Dearborn, Michigan, October 21–24, 1985, Society of Automotive Engineers, Warrendale, Pa, pp. 165, 279–84.

Liu, K. C. & Brinkman, C. R. (1988). Dynamic tensile cyclic fatigue of $Si_3N_4$. In *Proceedings of the 25th Automotive Technology Development Contractors' Coordination Meeting*, Dearborn, Michigan, October 26–29, 1987, Society of Automotive Engineers, Warrendale, Pa., pp. 189–97, 209.

Nilsson, J. & Mattsson, B. (1986). A new tensile test method for ceramic materials. In *2nd Int. Symposium on Ceramic Materials and Components for Engines*, Travemunde, April.

Sharp, W. N. (1971). Interferometric surface strain measurement. *Int. J. Nondestructive Testing*, **3**, 59–76.

Soma, T., Matsui, M. & Oda, I. (1985). Tensile strength of a sintered silicon nitride. In *Int. Conf. on Non-oxide Technical and Engineering Ceramics*, Limerick, Ireland, July, Elsevier Applied Science, London.